Journal of Materials Chemistry A

PAPER

View Article Online
View Journal | View Issue

Cite this: J. Mater. Chem. A, 2015, 3, 4248

Thermodynamic complexity of carbon capture in alkylamine-functionalized metal–organic frameworks†

D. Wu,‡[a] T. M. McDonald,‡[b] Z. Quan,‡[c] S. V. Ushakov,‡[a] P. Zhang,‡[d] J. R. Long‡[b] and A. Navrotsky‡*[a]

Received 27th November 2014
Accepted 14th January 2015

DOI: 10.1039/c4ta06496h

www.rsc.org/MaterialsA

For coordinatively unsaturated metal–organic frameworks (MOFs), the metal centers can be functionalized as CO_2 capture/storage adsorbents by grafting species having specific active groups. We report direct measurement of enthalpy of adsorption of CO_2 on an alkylamine-appended MOF, mmen-Mg_2(dobpdc) employing gas adsorption calorimetry at 298, 323 and 348 K. This methodology provides, for the first time, the detailed dependence of energy and entropy of sorption as a function of coverage and temperature. The enthalpy data suggest three types of adsorption events: strongest exothermic initial chemisorption at low coverage, majority moderate chemisorption at intermediate loading and weakest physisorption at highest coverage. The partial molar properties and isotherms are consistent with the presence of two different potential chemisorption mechanisms: 2 : 1 (amine–CO_2) stoichiometry near zero coverage and 1 : 1 afterwards. Both chemical potential and differential enthalpy of adsorption become less negative with increasing temperature, implying increasing adsorbent entropy at elevated temperature. These observations are consistent with weaker CO_2 binding at higher temperature.

Introduction

To mitigate the effects of rising atmospheric CO_2 levels related to burning of fossil fuels, various strategies are being investigated to design and develop advanced materials to control and capture CO_2 emissions.[1,2] Current technologies emphasize CO_2 capture materials such as aqueous phase alkanolamine[3] and solid framework materials[4] including zeolite molecular sieves,[5,6] alkylamine-grafted silicas[7–9] and metal–organic frameworks (MOFs). MOFs represent a class of highly porous, crystalline, metal–organic hybrid materials which have promising adsorption/separation properties due to their high surface areas, extremely open internal void space and chemical tunability. They are built through coordination between metal cations and rigid organic linkers.[10] Once the metal cation clusters are partially coordinated, leaving empty orbitals, further alkylamine functionalization is applicable, which may greatly enhance CO_2 adsorption.[11–13] One model material is an alkylamine-appended MOF, mmen-Mg_2(dobpdc), (an expanded version of Mg-MOF-74 appended with *N*,*N*′-dimethylethylenediamine), developed by McDonald *et al.*,[14] which exhibits significantly improved carbon capture capability, steep gas uptake, unusual "S-shaped" isotherms[14] and potential complicated reaction mechanisms.[15] The prospect of functionalized MOFs as gas sorbents brings up a challenging scientific issue, namely, to obtain accurate descriptions of the energetics of adsorption for multi-site, strong chemisorption possessing a steep initial stage and/or hysteresis. In such complex cases, the traditional isosteric heat calculation using adsorption isotherms obtained at different temperatures can be problematic, in part because the functional form of equations used can not be constrained *a priori* and may indeed depend on temperature. In practical operation, energy efficient carbon capture from coal based power plants and natural gas streams requires adsorption at elevated temperature (usually above 313 K). Therefore, the energetic effects involved in these conditions are essential and crucial to understand and optimize an energy efficient CO_2 adsorption process. The calorimetric methodology in this study provides, for the first time, direct measurement of enthalpy of sorption as a function of coverage (including at very low gas loading) and temperature. Combining these calorimetric data and the adsorption isotherms enables accurate calculation of entropies of sorption. These thermodynamic

[a]Peter A. Rock Thermochemistry Laboratory and NEAT ORU, University of California, Davis, California, 95616, USA. E-mail: anavrotsky@ucdavis.edu

[b]Department of Chemistry, University of California, Berkeley, California, 94720, USA

[c]Earth and Environmental Sciences Division, Los Alamos National Laboratory, Los Alamos, New Mexico, 87545, USA

[d]School of Materials Science and Engineering, State Key Laboratory for Metallic Matrix Composite Materials, Shanghai Jiao Tong University, Shanghai, 200240, China

† Electronic supplementary information (ESI) available. See DOI: 10.1039/c4ta06496h

‡ D.W. and A.N. designed the research. T.M.M. and J.R.L. provide the material. D.W., Z.Q. and P.Z. performed the research. D.W., S.V.U. and A.N. analyzed the data. D.W. and A.N. wrote the paper.

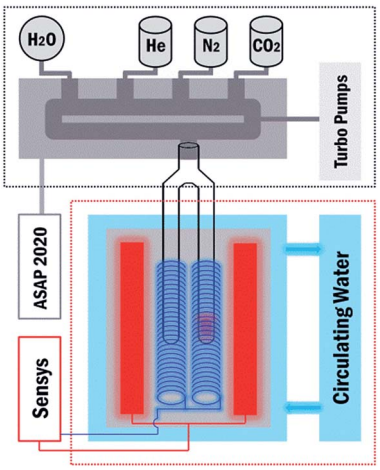

Fig. 1 Experimental apparatus for CO_2 adsorption calorimetry.

parameters provide insight into binding mechanisms and their variation with coverage and temperature.

The gas adsorption calorimetry system developed in the Peter A. Rock Thermochemistry Laboratory at UC Davis includes a Calvet-type microcalorimeter combined with a commercial gas dosing system (Fig. 1).[16] Our earlier adsorption calorimetry studies mainly focused on H_2O vapor adsorption on surfaces of nanoparticles and nanoporous media confining different guest cations or molecules.[17–20] Recently, we adapted this technique to explore the reaction mechanism of CO_2 adsorption on an environmental friendly sugar MOF (CD-MOF-2).[21] Strong exothermic heat effects at near zero coverage were directly obtained and different active adsorption sites of the material were mapped and assigned to specific bonding geometries. In this work, we utilize this methodology to investigate the enthalpy of CO_2 adsorption on an alkylamine-functionalized MOF, mmen-Mg_2(dobpdc). By performing direct enthalpy of adsorption measurements, we determine the enthalpy of gas adsorption as a function of CO_2 loading (mmol g^{-1} sorbent), the magnitude of the strong, initial binding at near zero gas coverage, adsorption reversibility, the proportion of major chemisorbed CO_2, and the enthalpy of adsorption at several temperatures. In light of these direct experimental observations, we interpret the mechanism of CO_2 adsorption and discuss the change of partial molar properties in the CO_2–mmen-Mg_2(dobpdc) system as a function of gas loading and of temperature. We conclude that CO_2 adsorption in mmen-functionalized Mg_2(dobpdc) is a complex process involving multiple thermodynamic factors reflecting changes in structure and bonding as temperature and gas loading vary.

Experimental methods

The detailed chemical and structural analyses of mmen-Mg_2(dobpdc), including both crystallographic information and powder X-ray diffraction patterns, have been published elsewhere[14] by some of the coauthors in the present work. So we do not repeat them here.

Small-angle X-ray scattering (SAXS) measurement of mmen-Mg_2(dobpdc) was conducted at B1 station of Cornell High Energy Synchrotron Source (CHESS) using an angle dispersive synchrotron X-ray technique to determine the material structure. Using a double crystal monochromator, the white X-rays were collimated into monochromatic beam at a wavelength of 0.485946 Å for SAXS measurement.[22] A large MAR345 detector was used to record the X-ray scattered signals from the sample. Using a Fit2D software, the two-dimensional (2D) images were integrated into one-dimensional (1D) patterns with intensity as a function of 2θ (degree) for structural analysis.

The enthalpies of CO_2 adsorption were measured by gas adsorption calorimetry (see Fig. 1) at 298, 323 and 348 K using a gas adsorption analyzer (Micromeritics ASAP 2020) coupled to a Calvet-type microcalorimeter (Setaram Sensys).[16] About 30 mg of mmen-Mg_2(dobpdc) was placed in one side of a custom-made silica glass forked tube, and the other side of the tube was left empty as a reference. This sample tube was placed into the twin chambers of the microcalorimeter, connected to the analysis port of ASAP 2020 and subjected to degas under vacuum ($<10^{-3}$ Pa) for 36 hours at 373 K to maximize the desorption of any initial adsorbates. The gas adsorption analyzer was set in incremental dosing mode (1 μmol per dose). To ensure equilibration, the time between each dose was 1.0–1.5 hour. In each experiment, the isotherm and associated heat effect were recorded simultaneously. Each dose of CO_2 resulted in a distinct calorimetric peak representing the heat effect generated by the adsorption of that dose. Volumetric detection of the amount of adsorbed CO_2 was recorded by the gas adsorption analyzer. Calisto Processing software (AKTS, Switzerland) was used to obtain enthalpies of adsorption (kJ per mol of CO_2). Between each set of adsorption measurements, the sample was regenerated at 373 K under vacuum overnight.

Three sets of calorimetric experiments were designed to investigate CO_2 adsorption mechanisms. First, reversibility of CO_2 adsorption was tested by performing the enthalpy of CO_2 adsorption measurements a second time after regeneration under vacuum at 373 K for 12 hours between the two sets of measurements. Then the following procedure was used to separate chemisorption from the whole adsorption event. Right after the second round of CO_2 adsorption (up to saturation) on fresh mmen-Mg_2(dobpdc) at 298 K, the same sample was degassed without heat treatment in the same forked tube, followed by a third round of adsorption calorimetry at 298 K. The purpose was to retain the chemisorbed CO_2 but remove the physisorbed CO_2 so that this round of calorimetry could not access the strong binding sites since they remained filled. Finally, enthalpies of CO_2 adsorption were measured at 298, 323 and 348 K. The absence of heat effects from dosing of CO_2 in calorimeter above 298 K was verified with experiment using silica glass in place of the sample. All the measurements were triplicated for reproducibility.

Results

The 1D integrated SAXS pattern is shown in Fig. 2. There are three detectable peaks with d-spacings of 1.86 nm (d1), 1.07 nm

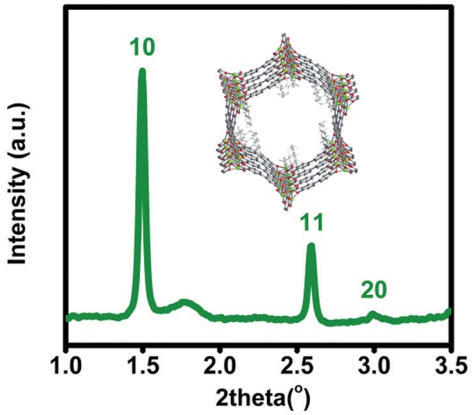

Fig. 2 Small-angle X-ray scattering (SAXS) pattern for mmen-Mg_2(dobpdc) and structure of mmen-Mg_2(dobpdc), green, red, and gray spheres denote Mg, O, and C atoms, respectively.

(d2), and 0.93 (d3) nm, respectively. Therefore, the corresponding ratios ($d1/dn$) are close to 1, $\sqrt{3}$, and 2, indicating a typical hexagonal superstructure. Combined with the nature of this mesoporous sample, the first three peaks are therefore indexed as (10), (11), and (20), respectively. It should be noted that this unique labeling is derived from the 2D hexagonal structure.[23] Therefore, the constant of the 2D hexagonal *meso*-structure lattice (a) was calculated to be 2.15 nm using the equation below:[23]

$$\frac{1}{d_{(\mathrm{hk})}{}^2} = \frac{4}{3} \times \frac{h^2 + hk + k^2}{a^2}$$

Fig. 3 presents the adsorption isotherms and associated differential enthalpy of adsorption curve for the first, second and third round of CO_2 adsorption. The measured enthalpies of adsorption are listed in Table 1. The isotherms and differential enthalpy of adsorption curves of the first and second round of adsorption overlap entirely. This reproducibility strongly suggests that, after regeneration, mmen-Mg_2(dobpdc) maintains its CO_2 adsorption capacity without decreasing selectivity, keeping the same number of strong adsorption sites. The most exothermic differential enthalpy of CO_2 adsorption at near zero coverage is -94.4 ± 2.8 kJ per mol of CO_2. This strongly exothermic heat effect complements previous work of McDonald *et al.*[14] by providing enthalpy of CO_2 adsorption at near zero coverage, which could not be calculated by fitting isotherms. The differential enthalpy of adsorption becomes less exothermic as more CO_2 is adsorbed. It reaches a plateau of -75.0 ± 2.2 kJ per mol CO_2, which is the enthalpy of adsorption for the majority of chemisorption sites. The current data on this plateau, which represents most of the adsorption, are in good agreement with both the calculated adsorption energy from simulation[15] (-69 kJ mol^{-1} CO_2) and the isosteric heat effect[14] (-71 kJ mol^{-1} CO_2). The data at lower and higher coverage capture detail not seen in any earlier experiments or calculations.

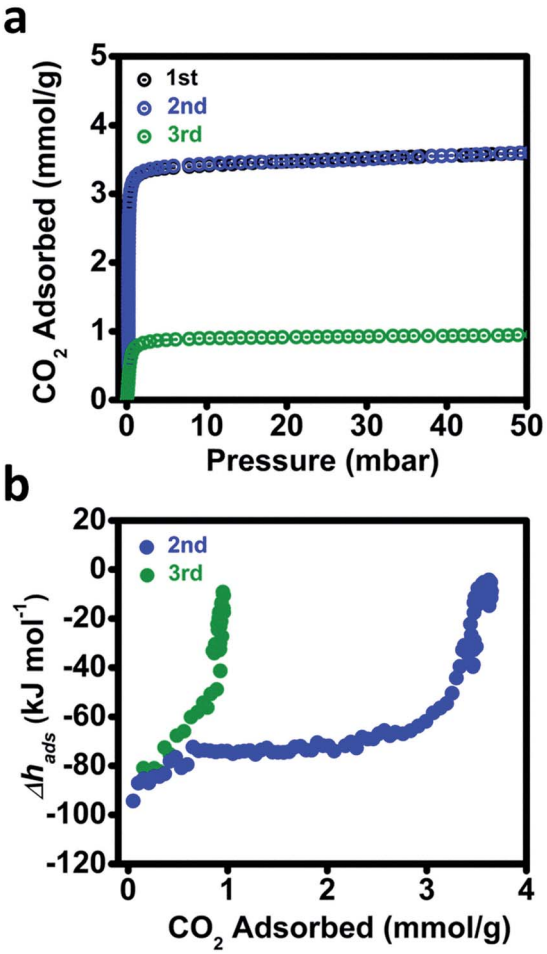

Fig. 3 (a) CO_2 adsorption isotherms at 298 K for the first (black) and second (blue) CO_2 adsorption round on the same mmen-Mg_2(dobpdc) sample (degassed at 373 K for 12 h after the first round). After the second round of CO_2 adsorption, the sample was subjected to degas without heating for 12 h at 298 K. Then the third round (green) CO_2 adsorption experiment was performed; and (b) differential enthalpies of CO_2 adsorption at 298 K for fresh mmen-Mg_2(dobpdc) (blue) and the same sample with major chemisorption on the plateau range inhibited (green).

The isotherm and enthalpies for the third round of adsorption represent readsorption of CO_2 which can be removed by strong vacuum at 298 K. The energetics suggests that this is mostly physisorption, with a possible small fraction of chemisorbed CO_2. Difference between this isotherm and those of fresh mmen-Mg_2(dobpdc) (first and second round) represents CO_2 bound on the major chemisorption sites (the plateau).

Table 1 Differential enthalpies of CO_2 adsorption at near zero coverage and major chemisorption only at 298, 323 and 348 K

Temperature (K)	$\Delta h_{\text{ads-zero coverage}}$ (kJ per mol CO_2)	$\Delta h_{\text{ads-chemi}}$ (kJ per mol CO_2)
298	-94.4 ± 2.8	-75.0 ± 2.2
323	-82.3 ± 4.1	-61.8 ± 3.6
348	-71.8 ± 4.0	-52.0 ± 5.4

When the pressure is 1.0 mbar, the amount of this chemisorbed CO_2 is about five times that of CO_2, which can be removed by vacuum. The differential enthalpy of adsorption curve in the third round (see Fig. 3b) shows no plateau representing the major chemisorption because the chemisorbed CO_2 is already present. As soon as the adsorption passes the stage of very small amounts of added CO_2, the curve directly passes into physisorption behavior.

To further elucidate complex CO_2 adsorption mechanisms, the partial molar properties of CO_2 adsorption and the isotherm at 298, 323 and 348 K are plotted *versus* the amount of CO_2 adsorbed per gram of mmen-Mg_2(dobpdc) in Fig. 4 (also see Fig. S1†). Pure gas phase CO_2 at 1 atm is selected as the standard state at each temperature. Chemical potential (partial molar free energy) curves are obtained directly from the adsorption isotherm, $\Delta\mu_{CO_2}$ (gas phase) $= RT\ln(p/p^o)$, $p^o = 1$ atm. In the pressure and temperature range investigated, the fugacity coefficient of CO_2 is very close to 1, so CO_2 can be considered to be an ideal gas whose enthalpy does not depend on pressure at constant temperature, so the only enthalpy term is that arising from adsorption. The partial molar entropy of adsorption is derived by using the relation $\Delta\mu = \Delta h - T\Delta s$. Specifically, all the isotherms exhibit signature steps with the switch points shifting to higher pressure as temperature increases (Fig. 4a). Chemisorption of CO_2 at higher temperatures yields less exothermic differential enthalpies, also supported by the upward shifted plateaus shown in Fig. 4b. Similar trends are also found on the $\Delta\mu_{ads}$ plots (Fig. 4c). For a given temperature, the chemical potential change becomes less negative as adsorption proceeds, reflecting the change in enthalpy and entropy, and indicating decreasing sorbent binding (less favorable reaction). The chemical potential curves exhibit similar temperature dependence as the differential enthalpy, with $\Delta\mu_{ads}$ showing less negative values at higher temperature for a fixed CO_2 loading. The temperature dependence of chemical potential and partial molar enthalpy is a strong indication of energetically less favorable adsorption at higher temperature. The entropy of adsorption becomes less negative with increasing temperature (Fig. 4d), also consistent with weaker binding at higher temperature. In addition, the standard state partial molar entropy of adsorption can be separated into terms arising from the pressure change and from

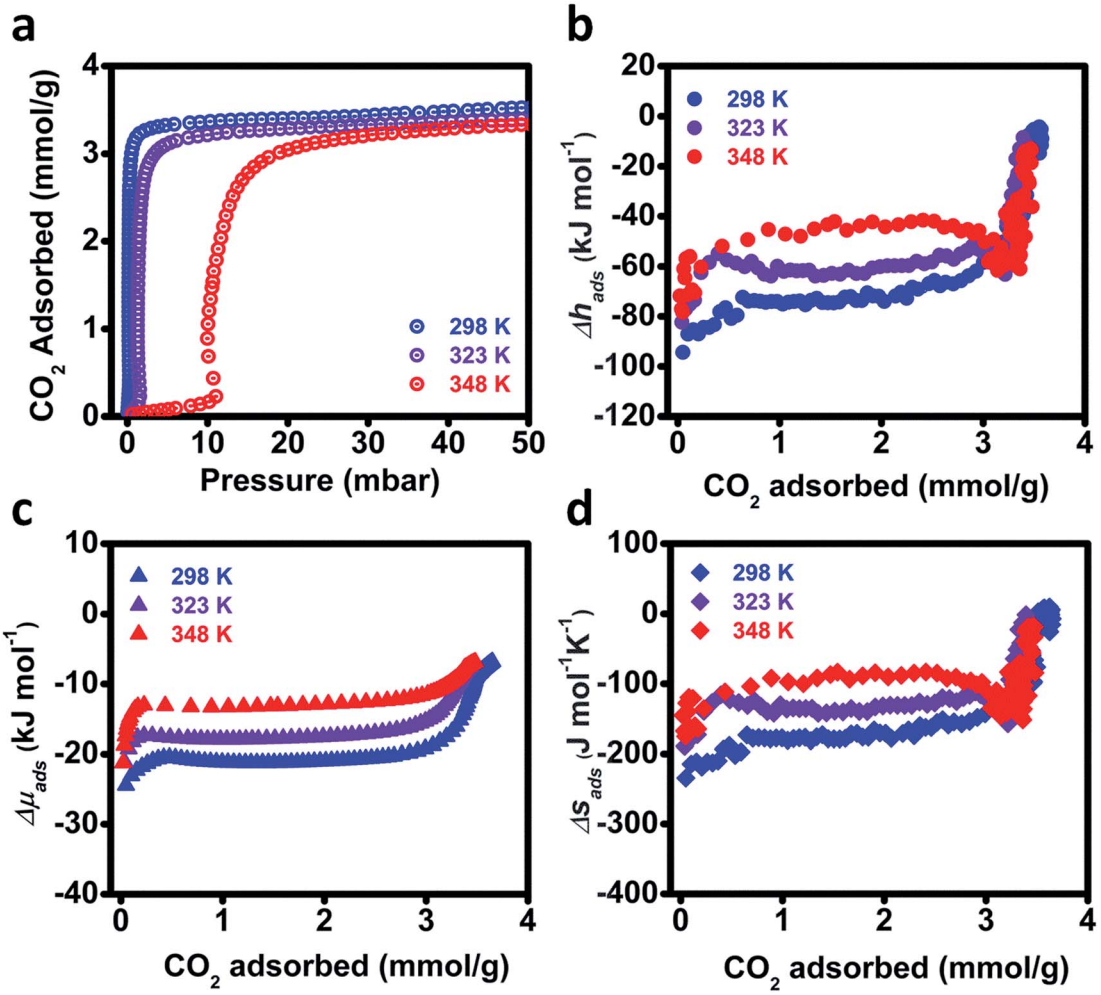

Fig. 4 (a) CO_2 adsorption isotherms and (b) corresponding differential enthalpies (c) free energies and (d) differential entropies of CO_2 adsorption curves at 298 (blue), 323 (purple) and 348 (red) K on the same mmen-Mg_2(dobpdc) sample.

adsorption. Each point of the isotherm (chemical potential curve) corresponds to adsorption equilibrium of CO_2 on mmen-Mg_2(dobpdc) at a specific temperature and pressure, in which the chemical potential of gas phase CO_2 is equal to that of the adsorbed molecules on the surface. Since in the experimental conditions investigated CO_2 can be treated as ideal gas, the chemical potential relations for adsorption equilibrium is represented by the equations below, where the reference state for CO_2 is taken as the ideal gas at 1 atm and the given temperature.

$$\Delta\mu_{CO_2}\,(\text{gas phase}) = RT\ln(p/p^{o}),\ (p^{o} = 1\ \text{atm}) \quad (1)$$

$$\Delta\mu_{CO_2}\,(\text{adsorbed}) = \Delta h_{CO_2}\,(\text{adsorbed}) - T\Delta s_{CO_2}\,(\text{adsorbed}) \quad (2)$$

$$\Delta\mu_{CO_2}\,(\text{gas phase}) = \Delta\mu_{CO_2}\,(\text{adsorbed}) \quad (3)$$

$$RT\ln p = \Delta h_{CO_2}\,(\text{adsorbed}) - T\Delta s_{CO_2}\,(\text{adsorbed}) \quad (4)$$

$$\Delta s_{CO_2}(\text{adsorbed}) = \frac{\Delta h_{CO_2}(\text{adsorbed})}{T} - R\ln p \quad (5)$$

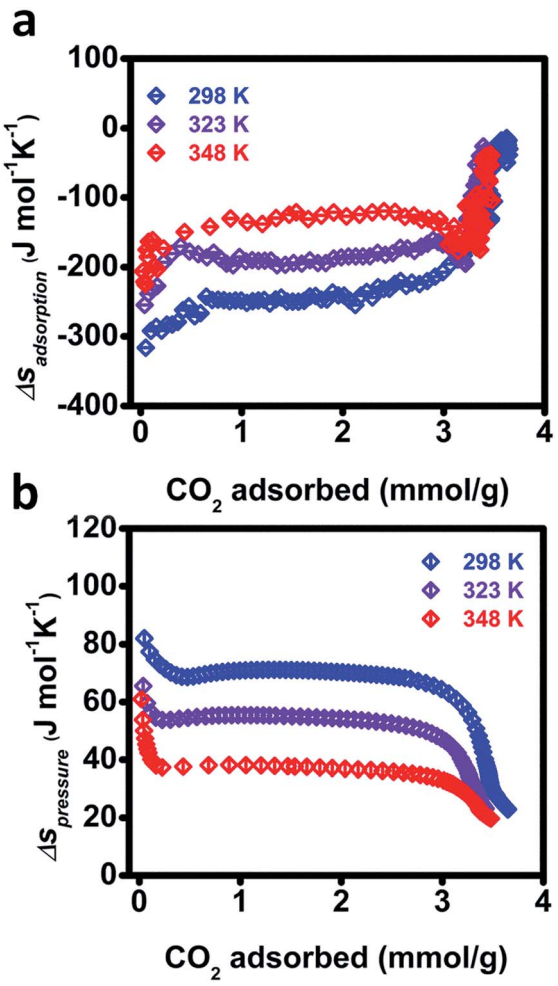

Fig. 5 Entropies of CO_2 adsorption at 298 (blue), 323 (purple) and 348 (red) K on the same mmen-Mg_2(dobpdc) sample, (a) contribution from CO_2 adsorption, (b) contribution from CO_2 expansion from 1 atm to the pressure in the adsorption isotherm.

Therefore, the partial molar entropy change associated only with the binding of CO_2, can be derived as $\Delta s_{adsorption} = \Delta h_{CO_2}$ (adsorbed)/T, (see Fig. 5a), and $\Delta s_{adsorption}$ shows the same trend as the differential adsorption enthalpy. On the other hand, the entropy contribution from pressure variation ($\Delta s_{pressure} = -R\ln p$) is shown in Fig. 5b. It becomes less positive at a given loading as temperature increases because at higher temperature a higher pressure is needed for a given coverage. Both chemisorption and physisorption of CO_2 are reproducible with regeneration at 373 K; adsorption is reversible and the MOF does not degrade upon regeneration.

Discussion

The enthalpies of sorption at room temperature in the plateau region, representing chemisorption, which accounts for most of the adsorption, are in the same range as previous values from both isosteric heat calculated from the temperature dependence of adsorption isotherms[14] and quantum-chemical calculations.[15] Direct gas adsorption calorimetry provides additional resolution in describing chemisorption of CO_2 on fresh, zero coverage material at various temperatures and at low and high coverage. Such sensitivity and resolution is not provided by the prior studies and indeed those methods can not readily discern the dependence of adsorption on coverage and temperature.

The partial molar properties (Δh_{ads}, $\Delta\mu_{ads}$, Δs_{ads}) and their corresponding isotherms at all three temperatures show clear evidence of discontinuity or at least of very rapid change over a small interval of coverage when plotted against the loading of CO_2 (Fig. 4). The sharp changes and plateaus on these curves divide each adsorption event into three distinct stages, the strongest exothermic initial adsorption, the majority moderate chemisorption at intermediate coverage and the weakest physisorption at highest coverage. Indeed, these discontinuous steps are strong indication of changing adsorption mechanisms, perhaps representing the occupation of distinct families of adsorption sites. Most previous reports suggest a 2 : 1 (amine–CO_2) reaction stoichiometry.[8,15,24] More recently, quantum-chemical calculations[15] demonstrate a 1 : 1 amine–CO_2 stoichiometry with a higher adsorption capacity as well as weaker adsorption energy than that of the 2 : 1 stoichiometry. In light of the current calorimetric observations, a multi-step reaction mechanism as a function of amount of CO_2 adsorbed is proposed. When the first dose is introduced, the local pressure of CO_2 in the pores of mmen-Mg_2(dobpdc) is extremely low. In other words, the population of amine groups on the pore surfaces is significantly higher than the very few CO_2 molecules inside the pores. Therefore, at this initial stage of chemisorption, a 2 : 1 stoichiometry is very likely to be favored, producing the most exothermic heat effect, supported by the S-shape step observed on the isotherm. Later on the isotherm, as more CO_2 molecules are deposited into the channels and adsorbed, fewer amine groups are available. Subsequently, when about 0.5 mmol g^{-1} CO_2 is loaded, the chemisorption appears to change sharply, probably to a 1 : 1 stoichiometry representing the lowest free energy (see the free energy plateau in Fig. 4c). Such evolution is reflected in both the enthalpy curves and isotherms. Therefore, it

is reasonable to have an S-shaped isotherm with stronger initial binding that fades with increasing coverage as the mechanism of binding changes. Furthermore, the most exothermic heat effects at low concentration with the 2 : 1 mechanism also have the most negative binding entropy, so the switch in mechanism reflects a competition between energetic and entropic factors. The calorimetric data support a sharp change in adsorption mechanism with loading but do not of themselves identify the microscopic structural details. Further structural and spectroscopic evidence is necessary to reveal and describe the reaction pathway on the molecular level.[25] Interestingly, for CO_2 adsorption at 323 and 348 K, the enthalpy of adsorption tends to be slightly more exothermic near the end of the plateau, before the start of physisorption. Although there is not clear spectroscopic evidence, it is possible that at high coverage and elevated temperatures the surface structure may undergo some rearrangement. This has not been investigated in detail as the overall effect is small.

Although a less exothermic enthalpy of adsorption with significant change of magnitude as temperature increases is not commonly observed for typical inorganic materials, the observed trend of chemisorption enthalpy for this MOF is entirely possible, since the organic functional groups of hybrid materials have additional degrees of freedom from vibration, rotation, and/or changing hydrogen bonding environments. In addition, the inherent flexibility of MOF type hybrid materials may contribute to the entropy term. Moreover, upon heating, the adsorption and desorption rates tend to increase dramatically approaching a point, at which the CO_2 mass transfer at gas/solid interface reaches dynamic equilibrium, with a significant number of molecules moving on the surface (Fig. 5). The above factors may make the energy of adsorption less favorable but increase the entropy of the system, as observed in this work.

The present thermodynamic study highlights several outstanding features of mmen-functionalized Mg_2(dobpdc) compared with traditional amine based MOF CO_2 sorbents. First, its unique "S-shaped" isotherm followed by steep uptake endows it with a large adsorption capacity at room temperature, a high chemisorption to physisorption ratio, and considerable binding strength. This enhances the capacity, selectivity, and stability during storage and transportation of a CO_2 loaded MOF. In addition, the decreased magnitude of heat effects at higher operating temperature may make desorption easier and reduce energy cost in sorbent regeneration. Furthermore, this study also implies that the entropic contribution at elevated temperature is significant and hence may have to be considered for optimization of applications. The present study is a first step and emphasizes the fundamental physical chemistry of interaction between the mmen-Mg_2(dobpdc) and CO_2, without overcomplicating the system with additional components. In future optimization of the industrial application of CO_2 capture sorbents, H_2O vapor, SO_x, and NO_x, should also be considered.

Conclusions

Direct gas adsorption calorimetry of CO_2 on mmen-Mg_2(dobpdc) determined the binding energies as a function of loading, tested the capture reproducibility and reversibility, separated and quantified the different types of binding sites, and suggested reaction mechanisms in different loadings at different temperature. These detailed findings are a crucial first step to design and optimize new carbon capture materials. Future research will focus on expanding thermodynamic study of carbon dioxide adsorption at various temperatures, and on hydrated functionalized MOF surfaces, providing essential information for MOF-based CO_2 adsorbents in real operating conditions.

Acknowledgements

The calorimetric work was supported by the U.S. Department of Energy, Office of Basic Energy Sciences, Grant DE-FG02-05ER15667. The Cornell High Energy Synchrotron Source is supported by National Science Foundation Award DMR-0936384. Other work related to this study received support from the Center for Gas Separations Relevant to Clean Energy Technologies, an Energy Frontier Research Center funded by the U.S. Department of Energy, Office of Science, Office of Basic Energy Sciences, under Award DE-SC0001015.

References

1 R. Quadrelli and S. Peterson, *Energy Policy*, 2007, **35**, 5938–5952.
2 S. Chu, *Science*, 2009, **325**, 1599.
3 G. T. Rochelle, *Science*, 2009, **325**, 1652–1654.
4 Q. A. Wang, J. Z. Luo, Z. Y. Zhong and A. Borgna, *Energy Environ. Sci.*, 2011, **4**, 42–55.
5 J. Kim, L. C. Lin, J. A. Swisher, M. Haranczyk and B. Smit, *J. Am. Chem. Soc.*, 2012, **134**, 18940–18943.
6 L. Espinal, W. Wong-Ng, J. A. Kaduk, A. J. Allen, C. R. Snyder, C. Chiu, D. W. Siderius, L. Li, E. Cockayne, A. E. Espinal and S. L. Suib, *J. Am. Chem. Soc.*, 2012, **134**, 7944–7951.
7 J. C. Hicks, J. H. Drese, D. J. Fauth, M. L. Gray, G. G. Qi and C. W. Jones, *J. Am. Chem. Soc.*, 2008, **130**, 2902–2903.
8 A. Sayari, A. Heydari-Gorji and Y. Yang, *J. Am. Chem. Soc.*, 2012, **134**, 13834–13842.
9 J. P. Sculley and H. C. Zhou, *Angew. Chem., Int. Ed.*, 2012, **51**, 12660–12661.
10 T. R. Cook, Y. R. Zheng and P. J. Stang, *Chem. Rev.*, 2013, **113**, 734–777.
11 D. M. D'Alessandro, B. Smit and J. R. Long, *Angew. Chem., Int. Ed.*, 2010, **49**, 6058–6082.
12 K. Sumida, D. L. Rogow, J. A. Mason, T. M. McDonald, E. D. Bloch, Z. R. Herm, T. H. Bae and J. R. Long, *Chem. Rev.*, 2012, **112**, 724–781.
13 S. Couck, J. F. M. Denayer, G. V. Baron, T. Remy, J. Gascon and F. Kapteijn, *J. Am. Chem. Soc.*, 2009, **131**, 6326–6327.
14 T. M. McDonald, W. R. Lee, J. A. Mason, B. M. Wiers, C. S. Hong and J. R. Long, *J. Am. Chem. Soc.*, 2012, **134**, 7056–7065.
15 N. Planas, A. L. Dzubak, R. Poloni, L. C. Lin, A. McManus, T. M. McDonald, J. B. Neaton, J. R. Long, B. Smit and L. Gagliardi, *J. Am. Chem. Soc.*, 2013, **135**, 7402–7405.

16 S. V. Ushakov and A. Navrotsky, *Appl. Phys. Lett.*, 2005, **87**, 164103.
17 A. Navrotsky, L. Mazeina and J. Majzlan, *Science*, 2008, **319**, 1635–1638.
18 A. Navrotsky, C. C. Ma, K. Lilova and N. Birkner, *Science*, 2010, **330**, 199–201.
19 A. H. Tavakoli, P. S. Maram, S. J. Widgeon, J. Rufner, K. van Benthem, S. Ushakov, S. Sen and A. Navrotsky, *J. Phys. Chem. C*, 2013, **117**, 17123–17130.
20 C. C. C. Gustavo, P. S. Maram and A. Navrotsky, *Angew. Chem., Int. Ed.*, 2013, **52**, 12139–12142.
21 D. Wu, J. J. Gassensmith, D. Gouvea, S. Ushakov, J. F. Stoddart and A. Navrotsky, *J. Am. Chem. Soc.*, 2013, **135**, 6790–6793.
22 Z. W. Wang, O. Chen, C. Y. Cao, K. Finkelstein, D. M. Smilgies, X. M. Lu and W. A. Bassett, *Rev. Sci. Instrum.*, 2010, **81**, 093902.
23 T. Hahn, *Int. Tables Crystallogr.*, 1983, vol. A.
24 A. Sayari and Y. Belmabkhout, *J. Am. Chem. Soc.*, 2010, **132**, 6312–6314.
25 Spectroscopic and structural studies, which support our thermodynamic conclusions, have been carried out parallelly by some of the coauthors in this work. A separated paper has been submitted to elsewhere.

